Int J Biometeorol (2004) 49:113–129
DOI 10.1007/s00484-004-0214-6

ORIGINAL ARTICLE

K. Kubaha · D. Fiala · J. Toftum · A. H. Taki

Human projected area factors for detailed direct and diffuse solar radiation analysis

Received: 3 October 2003 / Revised: 28 April 2004 / Accepted: 19 May 2004 / Published online: 20 July 2004

Abstract Projected area factors for individual segments of the standing and sedentary human body were modelled for both direct and diffuse solar radiation using detailed 3D geometry and radiation models. The local projected area factors with respect to direct short-wave radiation are a function of the solar azimuth angle (α) between $0°<\alpha<360°$ and the solar altitude (β) angles between $-90°<\beta<+90°$. In case of diffuse solar radiation from the isotropic sky the local human projected area factors were modelled as a function of the ground albedo (ρ) ranging between $0<\rho<1$. The model was validated against available experimental data and showed good general agreement with projected area factors measured for both the human body as a whole and for local quantities. Scientists can use the equations to predict the inhomogeneous irradiation and absorption of direct and diffuse solar radiation and UV-radiation at surfaces of the human body. In conjunction with detailed multi-node models of human thermoregulation the equations can be used to predict the physiological implications of solar radiation and outdoor weather conditions on humans.

Keywords Solar radiation · Human radiation geometry · UV-dose · Outdoor climate · Modelling

K. Kubaha · D. Fiala (✉)
Institute of Energy and Sustainable Development,
De Montfort University,
Leicester, UK
e-mail: dfiala@dmu.ac.uk
Tel.: +44-116-2577971
Fax: +44-116-2577981

J. Toftum
International Centre for Indoor Environment and Energy,
Technical University of Denmark,
Lyngby, Denmark

A. H. Taki
School of Architecture,
De Montfort University,
The Gateway, Leicester, UK

Introduction

Radiative heat exchange with the environment plays an important role in the human heat transfer and thermal comfort. In buildings, occupants are frequently exposed to inhomogeneous radiation, e.g. in the proximity of cold windows, hot radiators, or due to solar radiation transmitted through glazed façades. Such asymmetric conditions can make indoor environments thermally uncomfortable, cause restrictions in the usability and functionality of spaces and reduce occupants' productivity in the work place. In cars and aircraft cabins such uncomfortable conditions can slow down the reactions of drivers and pilots. Critical, life-threatening situations arise for people such as firefighters on duty or workers in metal work factories who are exposed to thermal radiation from fire and intense heat.

Outdoors, both direct and diffuse solar radiation can reach levels at which the impact on human thermal comfort and the perceived outdoor temperature is overwhelming. Besides perceptual effects, there are various health implications of human exposure to solar radiation that require a careful consideration, Kimlin et al. (2002). Thereby, a detailed knowledge of the human radiant geometry and its local characteristics is required in cases where the risk of skin injury arises. The risk of injury due to overdose of UV-radiation, for example, depends on the local radiation geometry of exposed body parts rather than on global quantities. Despite the need for local characteristics, however, only the overall radiation data for the human body as a whole is available.

The amount of solar radiation received by a person depends on the projected area factor (f_p) as a geometry-related, direction-dependent radiation parameter of the human body. Over decades the human projected area factors and solar heat load have been subject to various experimental investigations. Underwood and Ward (1966), e.g. measured projected area factors of 25 standing male and female persons using photographic methods. The authors developed empirical formulae for predicting the f_p-factors of the human body as a whole

based on measurements obtained for seven different altitudes and three azimuth angles.

Fanger (1970) carried out extensive experimental trials to determine the projected area factors of 20 male and female subjects in the standing and sedentary position for azimuth and altitude angles between 0° to 180° and 0° to 90°, respectively. In these experiments, the camera was positioned at a relatively large distance (about 7 m) from the subjects to simulate the case of parallel rays from direct solar radiation. The original results were presented in form of graphs. Other authors (e.g. Steinman et al. 1988; Rizzo et al. 1991) have used Fanger's data to developed formulae for calculating the human projected area factors for use in computerised procedures. More recently, Jones et al. (1998) measured projected area factors of a full-scale manikin for a range of azimuth and altitude angles between $0°<\alpha<180°$ and $-90°<\beta<+90°$ (referring to the centre of the body) using a similar method employed by Fanger. The distance between the camera and the manikin however was set at 4.3 m and 3.7 m for positive and negative altitude angles, respectively. In contrast to other experiments, Jones et al. (1998) did not only measure the overall projected area factors of the body as a whole but also provided local quantities for individual body segments. Also alternative approaches to projected area factor concept to calculate solar heat load on human body have been developed by various authors, e.g. Breckenridge and Goldman (1972), Blazejczyk et al. (1992). Blazejczyk (1996), for example, proposed equations for assessing the amount of solar radiation absorbed by man using basic meteorological parameters.

To date, sophisticated computer simulation software tools are available which make detailed modelling of the human radiative heat exchange with the surrounding environment possible. There is a growing interest to predict human physiological and perceptual responses in various disciplines of science and technology, and, over decades, several multi-segmental models of the human thermal system (e.g. Stolwijk 1971; Fiala et al. 1999, 2001, 2003; Huizenga et al. 2001) have emerged that enable the effect of wide-ranging environmental conditions on human beings to be quantified. In recent years also software have become available using which detailed 3D models of the human body geometry can be generated for almost any body posture. Diverse CFD packages and thermal analysis tools are capable of predicting radiation exchange dealing with highly complex and boundary conditions geometries (such as the human body).

The level of detail and the accuracy in prediction make today's numerical radiation models superior to experimental investigations in several respects. There are hardly any restrictions regarding the considered geometrical configurations; the simulations can be run with the high intensity source at an infinite distance from the human body for any solar angle that can be exactly adjusted. In addition to direct radiation, it is also possible to study diffuse solar radiation effects for which no experimental results seem to exist. Predictions include detailed information on the solar irradiation mapping over the three dimensional human body surface. Besides overall body data, it is thus possible to obtain information also on the effect of local body characteristics which is required for detailed human radiation analysis.

Over the past years, several studies of the human radiative heat exchange have been carried out using numerical methods. Miyazaki et al. (1995), for example, considered the human body as consisting of several cylindrical parts and verified measured effective radiation area factors of the human body using the Monte Carlo method. Tanabe et al. (2000) used realistic 3D geometry models and solar heat gain calculations to predict projected area factors with respect to direct solar radiation for sedentary and standing subjects. As most experimental studies, however, overall human radiation data rather than local quantities were provided.

In this study numerical simulation techniques and detailed geometry models are used to predict projected area factors for individual segments of the human body. The aim of the work is to develop formulae for predicting local f_p-factors of standing and sedentary humans with respect to both direct and diffuse solar radiation that scientists and engineers can use to perform detailed shortwave radiation analysis, e.g. in conjunction with models of human thermoregulation, facial cooling and allowable exposure times, or models for predicting the UV-dose at exposed body parts.

Methodology

Human body models

The human body for both the standing and sedentary posture, was modelled as having left-right symmetry and a stress-free position using commercial software (Curious Labs 2000). The software enabled generating detailed 3D models of the human body for almost any body postures. Each model consisted of 10,995 small surface elements that provided sufficient detail for the radiation simulations (Fig. 1). With a height of 1.75 m and a DuBois' area of 1.83 m^2 this body size was felt as representing an average male subject, DuBois and DuBois (1916). The elements were grouped together into 19 main body parts (Table 1) subdivided into 59 spatial sectors (Fig. 2) for which the local projected area factors were to be modelled.

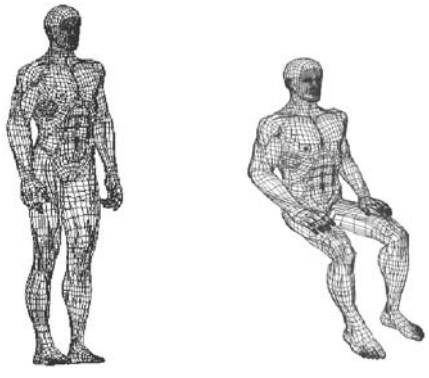

Fig. 1 The human body geometry models used in the study

Table 1 Surface areas of individual body sectors

Body parts	Body sectors	Surface area (m^2)
Head	Head	0.0525
	Forehead	0.005
Face	Anterior	0.0193
	Exterior (L/R)	0.011
Neck	Anterior	0.005
	Exterior (L/R)	0.0094
	Posterior	0.0068
Shoulder	Left	0.0205
	Right	0.0205
Thorax	Anterior	0.1115
	Inferior (L/R)	0.0093
	Posterior	0.0916
Abdomen	Anterior	0.1104
	Inferior (L/R)	0.0401
	Posterior	0.1091
Upper arm (L/R)	Anterior	0.0144
	Exterior	0.0292
	Inferior	0.0098
	Posterior	0.0143
Lower arm (L/R)	Anterior	0.0092
	Exterior	0.0269
	Inferior	0.0268
	Posterior	0.0124
Hand (L/R)	Handback	0.0285
	Palm	0.0276
Upper leg (L/R)	Anterior	0.0466
	Exterior	0.0503
	Inferior	0.0407
	Posterior	0.0386
Lower leg (L/R)	Lower anterior	0.0254
	Lower exterior	0.039
	Lower inferior	0.0335
	Lower posterior	0.0372
Foot (L/R)	Instep	0.04
	Sole	0.0203

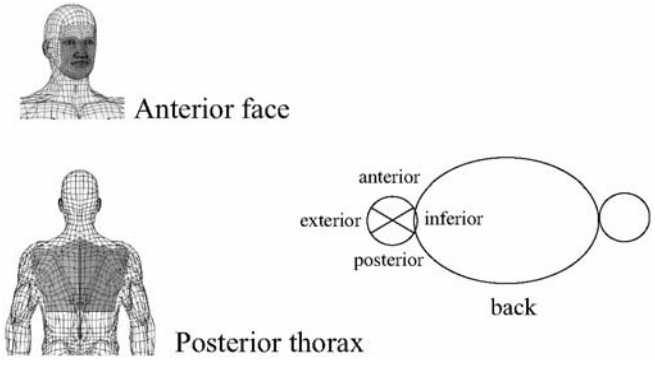

Fig. 2 Subdivision of the humanoid into individual body sectors

Radiation simulations

The humanoid geometries were imported into a thermal analysis software package (ThermoAnalytics 2001) which uses a voxel-based ray tracing technique to predict the absorbed short-wave radiation energy at each of the 10,995 surface elements. The scheme subdivides the scene to be ray-traced into small volume elements, or voxels. Rays were cast from each element to all other surrounding voxels and the high intensity source and the intersections were determined. The software calculated the amount of solar flux, $Q_{a,i}$, absorbed by each surface element from the incident solar radiation using the elements' short-wave absorptivities and the

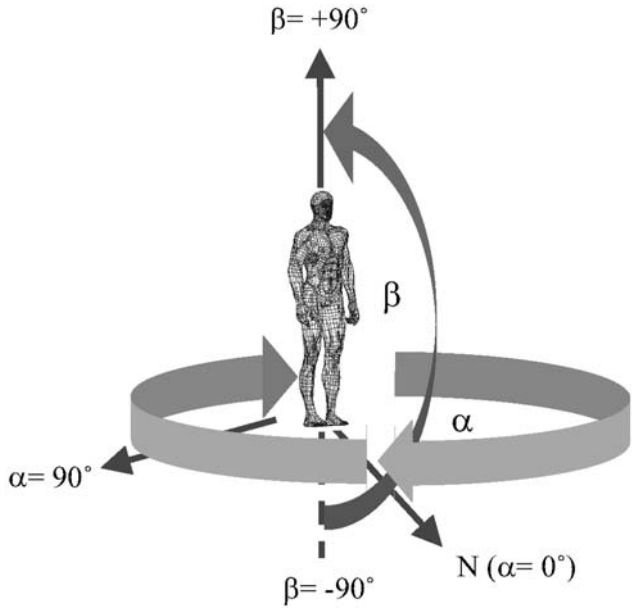

Fig. 3 Variation of the solar altitude (β) and azimuth angle (α) in the study

apparent areas predicted by the voxel based ray-tracing scheme. At this stage the surface elements were defined as black body radiators with an absorptivity of one to simplify the subsequent calculations. The results were then postprocessed integrating the elemental fluxes to obtain projected area factors for individual body sectors. Thereby, the total amount of short-wave radiation absorbed by a body sector consisting of n surface elements was obtained as the sum of predicted nodal quantities, $Q_{a,i}$. For a group of surface nodes, the projected area factor, f_p, which is defined as the ratio between the projected area and the actual surface area of a sector, is thus presented as

$$f_p = \frac{1}{q_s} \frac{\sum_{i=1}^{n} Q_{a,i}}{\sum_{i=1}^{n} A_i} \tag{1}$$

where f_p is the projected area factor of an individual body sector, $Q_{a,i}$ solar radiation absorbed by surface element i (W), q_s incident solar radiation flux (W/m^2), and A_i area of surface element i (m^2).

The projected area factors were calculated for both direct and diffuse short-wave radiation. For the direct short-wave radiation, the simulation procedure calculated the projected area factors across a range of azimuth angles, α, from 0° to 360° (due north, clockwise) and altitude angles, β, from −90° to 90° (Fig. 3). For the diffuse short-wave radiation case, the area factors were calculated by varying the ground albedo, ρ, between 0 and 1 (assuming isotropic, i.e. homogeneously radiating sky).

Regression analysis

Simple and polynomial regression was used to develop the equations. In case of direct solar radiation the f_p-factors were considered as functions of the solar azimuth and solar altitude angles α and β, and as functions of the ground albedo ρ in case of diffuse solar radiation. If any regression coefficient was not significantly different from zero at the 0.95 confidence level, a new regression was run without the non-significant variable. The two-tailed population t-test was applied to determine the significance level of the regression coefficients.

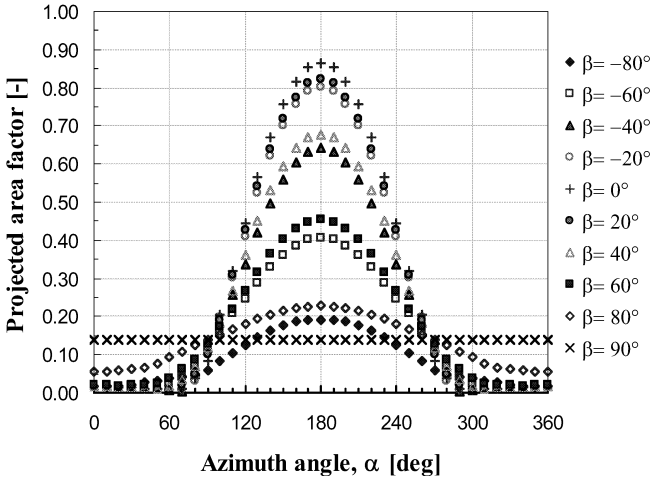

Fig. 4 The course of projected area factors predicted for the posterior thorax of a standing person

Modelling local projected area factors

Direct solar radiation

Analysis of the post-processed data indicated that for most parts of the human body the projected area factor curves for direct solar radiation (i.e. with respect to parallel rays) can be described as periodic, i.e. cosine or sine functions of the solar azimuth angle, α. As an example, the projected area factors predicted by the ray-tracing technique for the posterior thorax of a standing person are plotted in Fig. 4.

The trend of each curve can be commonly described using the following mathematical expression

$$f_p = A \cos(C_1\alpha + C_0) + B \tag{2}$$

where f_p=projected area factor of the body sector for a given β, α=azimuth angle (rad), C_1, C_0=regression coefficients

$$A = \frac{f_{p,max} - f_{p,min}}{2} \tag{3}$$

$$B = \frac{f_{p,max} + f_{p,min}}{2} \tag{4}$$

$f_{p,max}$=the maximum projected area factor, $f_{p,min}$=the minimum projected area factor.

The coefficients C_1 and C_0 were determined by regression analysis using a rearranged Eq. 2

$$\cos^{-1}\left(\frac{f_p - B}{A}\right) = C_1\alpha + C_0 \tag{5}$$

The coefficients A, B, C_0 and C_1 were not constant but varied depending on the solar altitude angle, β. As an example, these coefficients obtained for the posterior thorax are plotted against β in Fig. 5

The functions of these coefficients were determined using polynomials up to an order of four (see appendix, Tables 3, 4, 5).

In contrast to body parts that were fully exposed to the beam of direct radiation, Eq. 2 did not perform well for sectors that were hidden/partly hidden by other body parts at certain solar angles. As an example, in Fig. 6, such discrepancies between simulated data and f_p-factors pre-

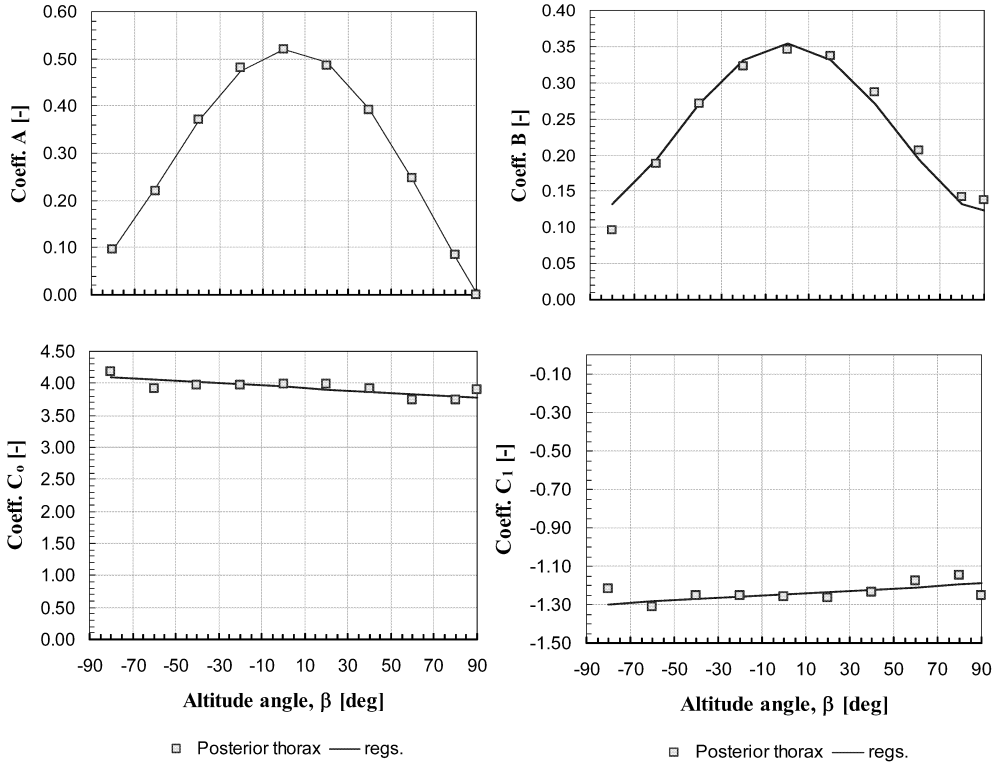

Fig. 5 The regression coefficients for the posterior thorax body sector

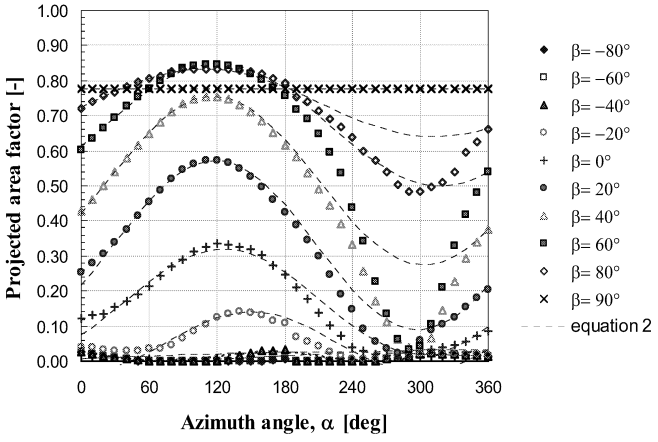

Fig. 6 Inadequacy of Eq. 2 to predict f_p-factors for sun positions where the body sector (right shoulder, standing posture) was hidden by another body part

dicted using Eq. 2 are apparent for azimuth angles $210°<\alpha<350°$ where the shoulder was "shaded" by the head.

It was, therefore, necessary to account for this "shading" effect by modelling the so called "shading-function" as a part of the final solution for each body sector. For this purpose, Eq. 2 was extended as follows

$$f_p = [A \cos(C_1\alpha + C_0) + B]S \tag{6}$$

where S is the shading function.

To model S, a number of different concepts were developed and tested. Thereby, the use of tanh functions turned out to be the most suitable approach

$$S = 1 + \frac{\tanh(D_1\alpha + D_0)}{2} + \frac{\tanh(E_1\alpha + E_0)}{2} \tag{7}$$

where D_1, D_0, E_1, and E_0 represent coefficients to be determined by regression analysis. Also these coefficients depended on the solar altitude, β, as shown for the shoulder body elements in Fig. 7. The results of the polynomial regressions for each coefficient are listed in appendix, Tables 6, 7, 8, 9.

Because of the symmetry of the humanoid models used in the study the results obtained for the right-hand body parts were applicable also to the left-hand side body element. For left-hand side body sectors, however, the reverse azimuth angle $\alpha^*=2\pi-\alpha$ has to be used with Eqs. 6, 7.

Diffuse solar radiation

In case of diffuse solar radiation the projected area factors, $f_{p,dif}$ could be described as linear functions of the ground albedo for each body part

$$f_{p,dif} = g_1\rho + g_0 \tag{8}$$

where $f_{p,dif}$ projected area factor of a body sector, ρ=ground albedo, g_0 and g_1 regression coefficients of individual body sector.

The results of the regression analysis are provided in Table 10.

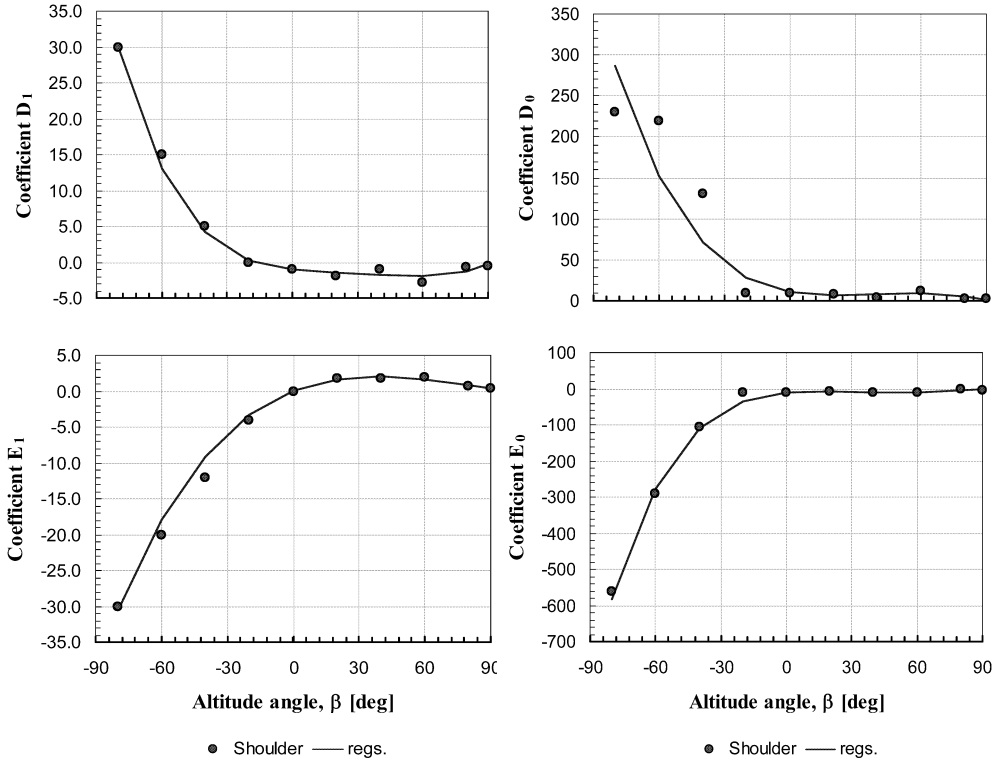

Fig. 7 The regression coefficients of the shading function for the shoulder body sector

Results

In the verification and validation process to which the new model was subjected, the predictions of the f_p-factors for each body sector of the standing and the sedentary human were first verified against simulation results obtained by the voxel-based ray tracing technique.

The results obtained for the head and the posterior thorax of the standing person exposed to the direct solar radiation are shown in Fig. 8. The irradiation of solar rays on both sectors was not obstructed by other body parts. In both cases the f_p-curves therefore exactly replicated the cosine function as described by Eq. 2. As can be seen, the predictions agreed well with the results of the ray-tracing simulations across the whole range of the azimuth and altitude angles, α and β.

Some, partly significant, deviations from the ideal cosine-shape trend are apparent from Fig. 9 in which the f_p-factors are plotted for the anterior face and the right shoulder. For the case of anterior face the upper legs of the sedentary posture hindered a full irradiation of solar rays on this body part causing a remarkable fall in f_p at a solar altitude of β=−60°. In case of the right shoulder the appreciable discrepancies from an ideal cosine-shape observed for $0°<\beta<60°$ between $210°<\alpha<330°$ were caused by the head. The shading function of the regression model accounted appropriately for these shadowing effects.

The analysis of the results indicated that for many body sectors, there was no or little effect of the body posture (i.e. standing and sedentary) on the local projected area factors. For other body parts, however, significant discrepancies occurred. Fig. 10 displays the differences

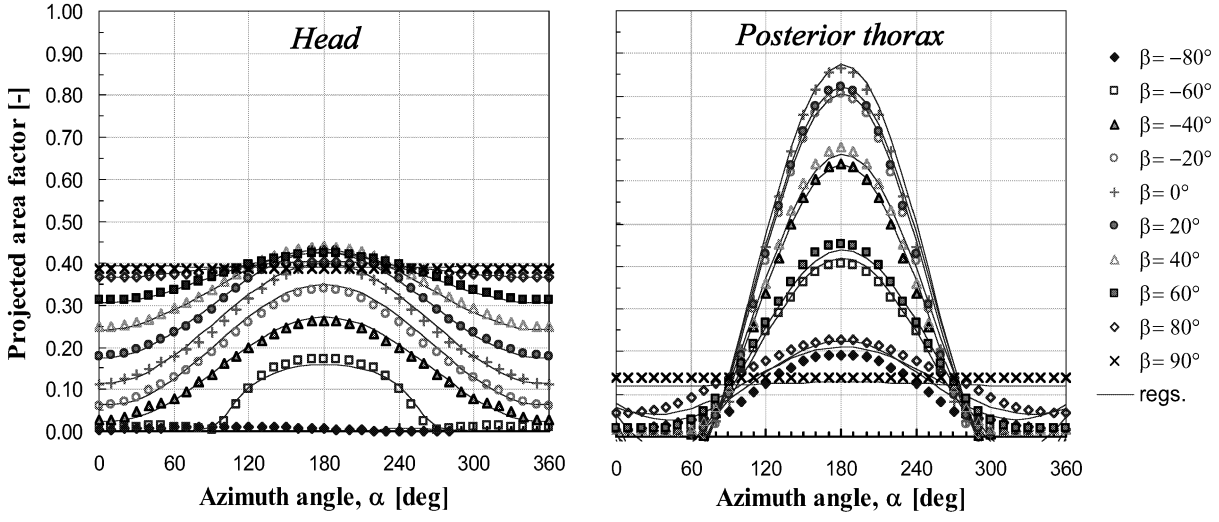

Fig. 8 Comparison of predicted and simulated projected area factor for two "unshaded" body parts, i.e. head (*left*) and posterior thorax (*right*) of the standing person

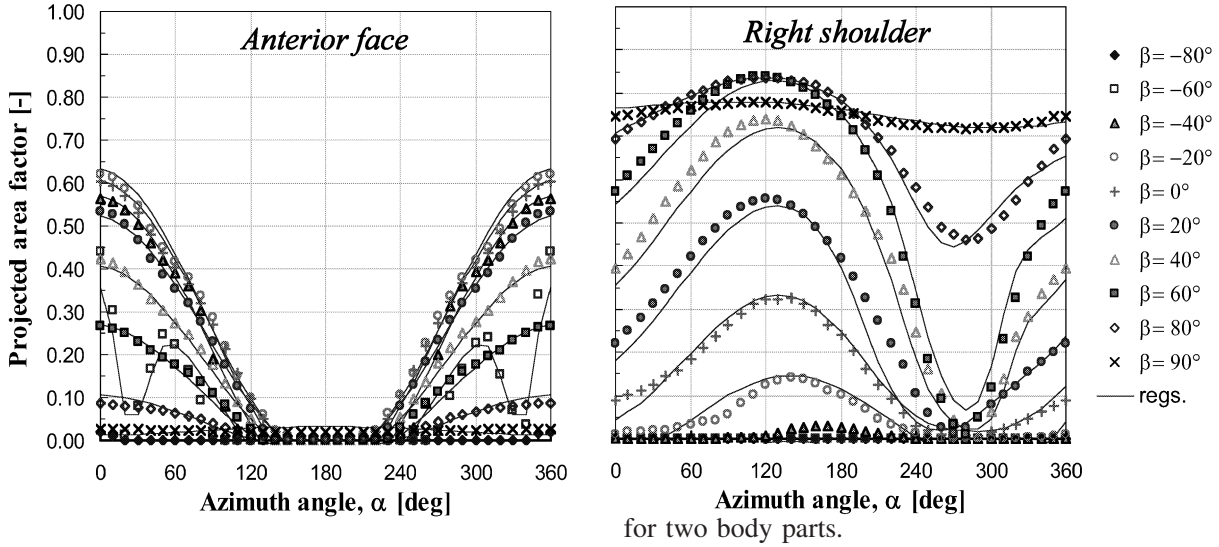

for two body parts.

Fig. 9 Effect of shadowing by other body parts on projected area factor of the anterior face (*left*) and the right shoulder (*right*) sector of a sedentary person

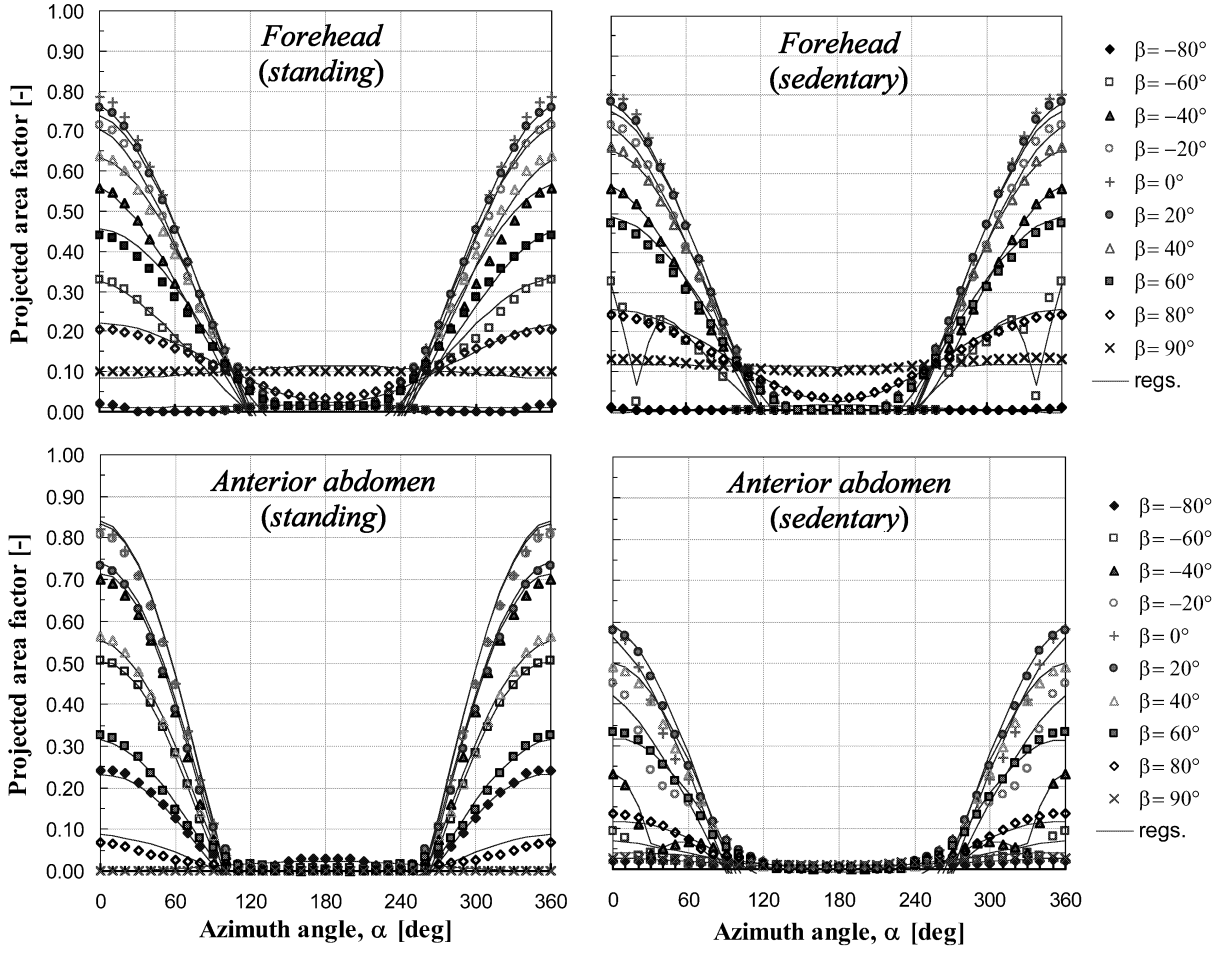

Fig. 10 The effect of body posture on the local projected area factors of the forehead and the anterior abdomen

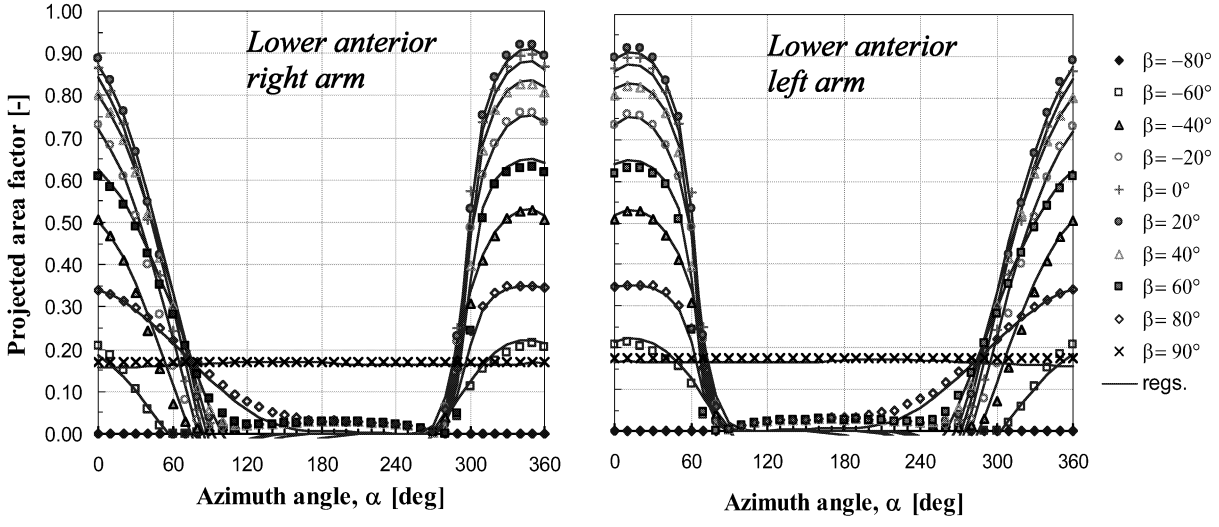

Fig. 11 Projected area factors of the right and left lower anterior arm predicted for a standing posture

For symmetry reasons, the local projected area factors were modelled explicitly only for the right-hand side body elements. The application of these regression results to both, the right and the left lower arm (anterior) is demonstrated in Fig. 11. As described previously the reverse azimuth angle $\alpha^*=2\pi-\alpha$ was used with Eqs. 6, 7 to predict the f_p-factors of the left hand-side body part in Fig. 11 (right).

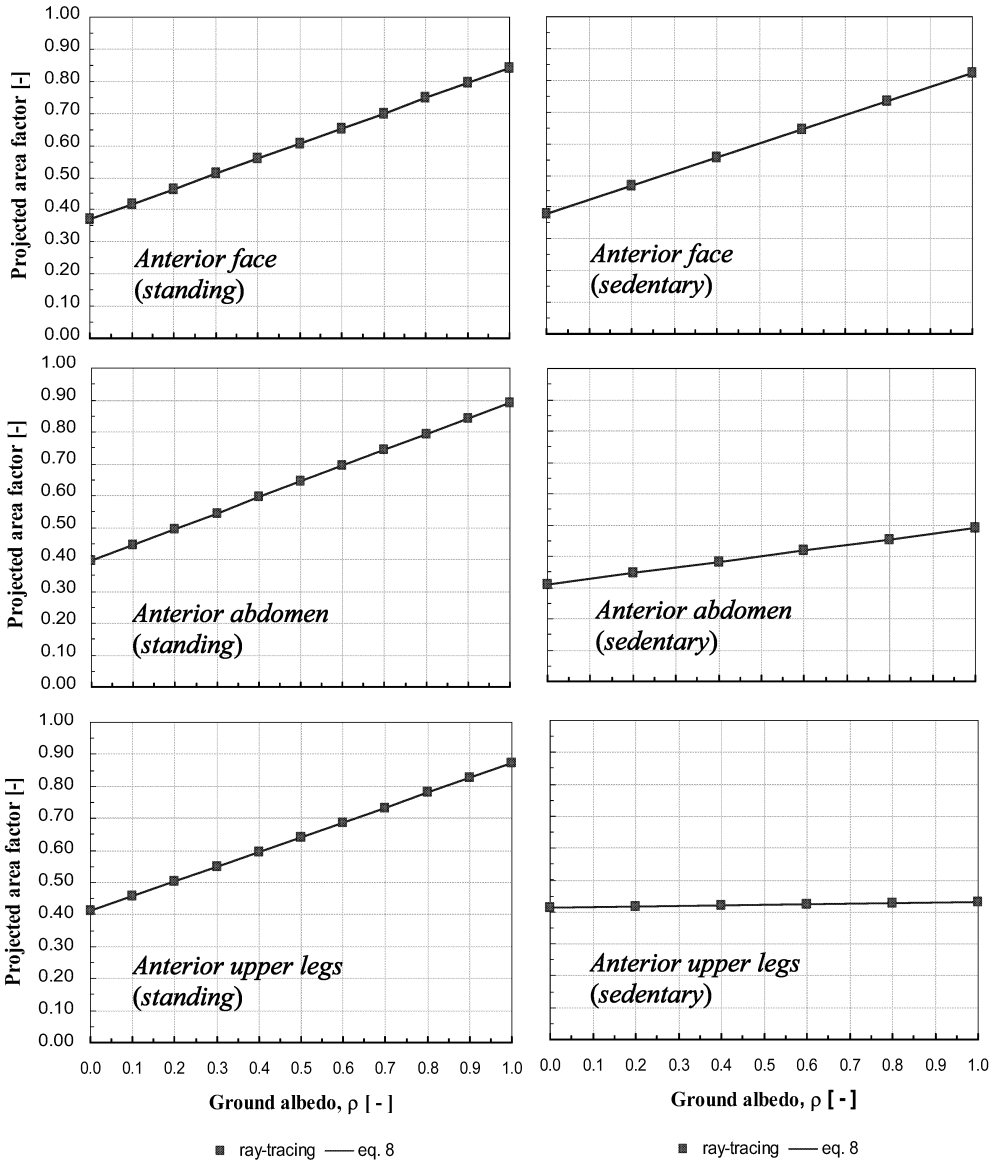

Fig. 12 Projected area factor curves for diffuse solar radiation of the anterior face (standing and sedentary), anterior abdomen (standing and sedentary) and upper anterior legs (standing and sedentary)

Finally, six examples for projected area factors with respect to diffuse solar radiation are shown in Fig. 12, indicating a linear relationship between $f_{p,\ dif}$ and the ground albedo, ρ, however with variable slopes. As in case of $f_{p,dif}$, there was little effect of the body posture for some body sectors (e.g. anterior face in Fig. 12). For other body parts, however, significant discrepancies occurred caused by changes in the orientation of individual body parts (e.g. anterior upper legs in Fig. 12) and/or shadowing effects through other body parts (anterior abdomen in Fig. 12).

Validation and discussion

To date, most experimental data is available just for the whole human body. To enable a comparison with these measurements, the predicted results obtained for individual body sectors were therefore integrated over the whole body surface. Furthermore, in most cases, experimental f_p-factors have been presented as a ratio of the projected body area and the effective radiation area (rather than the actual surface area). For validation purposes hence also the predicted values were weighted by the effective radiation area factor of the humanoid model used in this study (f_{eff}=0.84 and 0.78 for the standing and sedentary posture, respectively).

The results for the standing posture are compared with measured data obtained by Underwood and Ward (1966), Fanger (1970) and Jones et al. (1998) in Fig. 13. The marks indicate the experimental results whereas lines represent the predicted overall projected area factors as integrated over the humanoid's surface. Generally, the best agreement between predicted and measured values was achieved for the detailed experiments carried out by Fanger (1970). For most altitude and azimuth angles the discrepancy was typically about 5% relative error. Greater discrepancies resulted for the overall f_p-factors measured

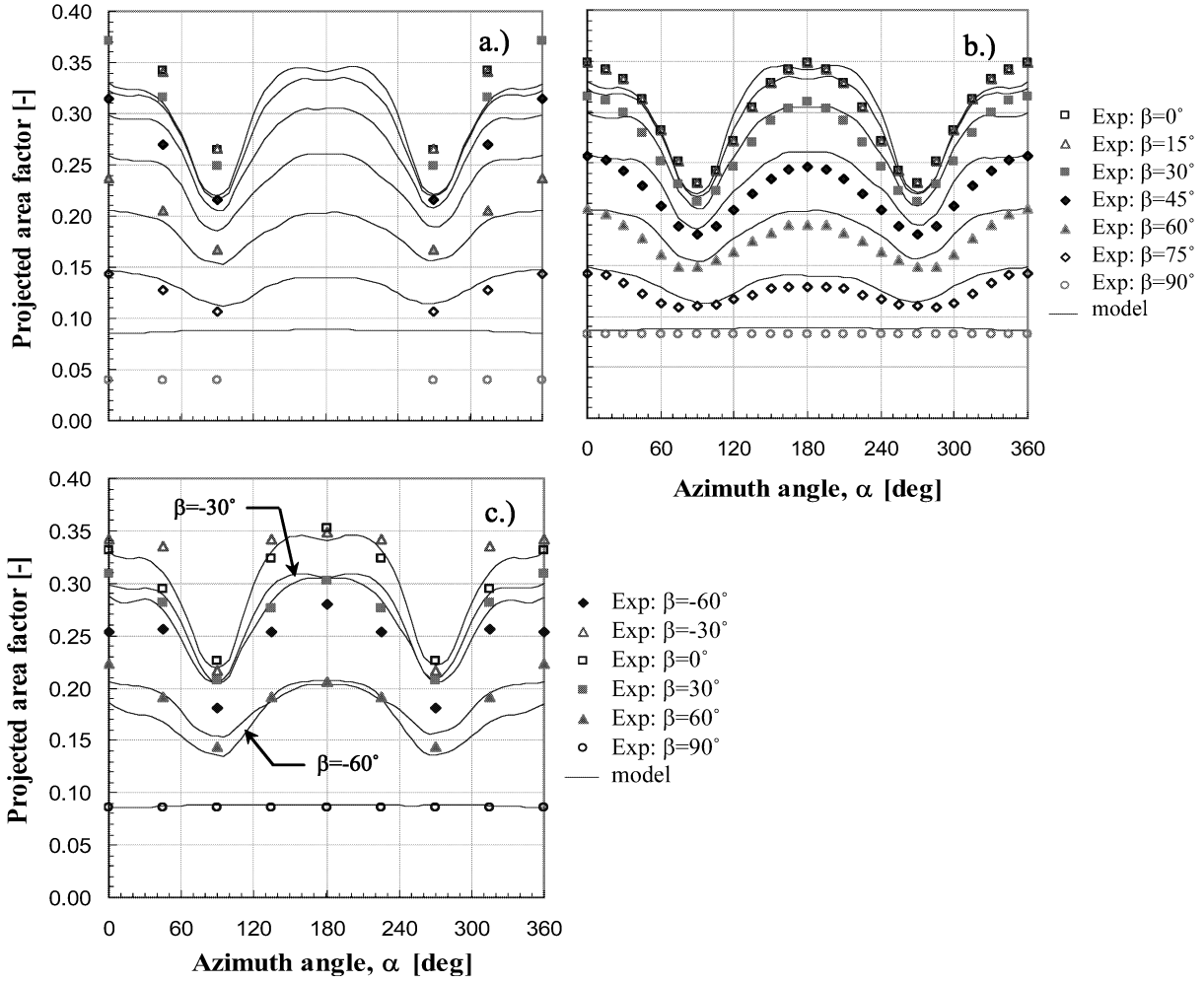

Fig. 13 Comparison of predicted projected area factors for the whole body in standing posture with experimental results obtained by: a) Underwood and Ward (1966), b) Fanger (1970), c) Jones et al. (1998)

by Jones et al. (1998) at β=–30° and β=–60°. For these altitude angles, however, the measured quantities were partly greater than for frontal exposures which seems less plausible and difficult to reproduce by rigorous numerical techniques. The lowest level of agreement resulted for the less detailed experiments of Underwood and Ward (1966) who measured the human f_p-factors for seven altitudes but only for three azimuth angles (0°, 45° and 90°). The largest discrepancy with twice as high predicted f_p-factors of Underwood and Ward resulted for β=90°. It should be noted that the effective radiation area of the subjects in the experiments was unknown and thus the f_{eff} of the humanoid model was used instead to weight the measured values in Fig. 13 representing a possible source of error.

The predicted overall projected area factors of the sedentary posture are compared against the experimental results of Fanger (1970) in Fig. 14. Similarly to the standing posture a good general agreement between prediction (solid lines) and experiment (data points) was obtained for most altitude and azimuth angles. An exception formed f_p-factors at an altitude angle of β=15° and α<60°/α>300° for which the discrepancy between

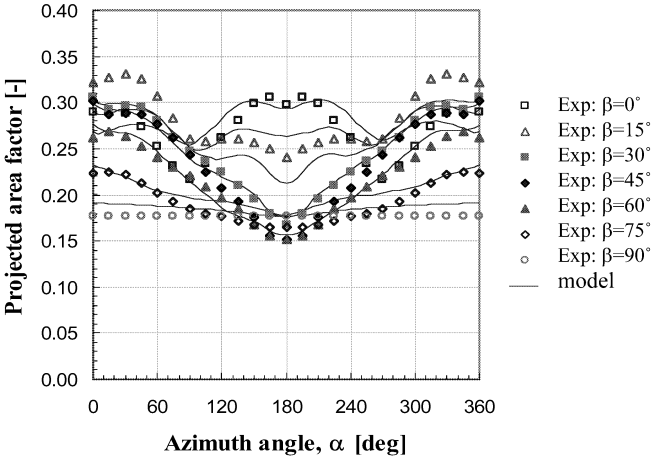

Fig. 14 Comparison of predicted overall projected area factors for the sedentary posture with experimental results obtained by Fanger (1970)

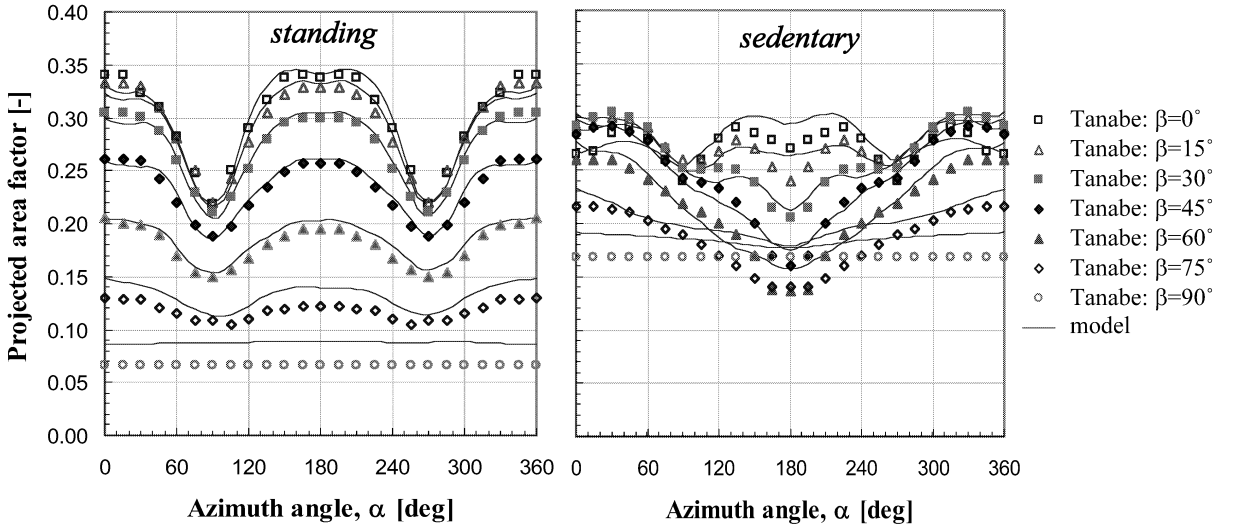

Fig. 15 Comparison of predicted projected area factors of the whole body with simulation results obtained by Tanabe et al. (2000)

prediction and measurement was greater than 10% relative error.

The results of this study were also compared with the simulation results obtained by other authors. A comparison with the overall projected area factors predicted by Tanabe et al. (2000) for standing and sedentary postures is shown in Fig. 15. The models agreed with each other within 7% relative error. The greatest relative discrepancies occurred at β=90° for both postures where the present regression model (which is based on more detailed geometry models) predicted the f_p-factors to be closer to the experimental results of Fanger (1970) than to the numerical results of Tanabe et al. (2000). It is interesting to note that this study confirmed the results of Tanabe et al. with respect to the maximum f_p-factors for α<60° and α>300° (sedentary posture) not exceeding 0.31 which contrasts the experimental results of Fanger with $f_{p,max}$=0.34.

In contrast to direct solar radiation no experimental data were found for f_p-factors with respect to diffuse solar radiation in the literature. Various authors (e.g. Fanger 1970; Horikoshi et al. 1990; Miyazaki et al. 1995; Tanabe et al. 2000), however, reported on measured effective radiation area factors for the human body as a whole. The effective radiation area factor is defined as the ratio between the effective radiation area and the actual surface area of the human body. Thereby, the effective radiation area is that area of the human body that is presented to the environment contributing to the radiation exchange with a diffusely radiating homogeneous enclosure. The experimentally observed human effective radiation area factors could therefore be directly compared with the predicted overall projected area factors obtained for diffuse radiation from the isotropic sky provided the ground albedo, ρ, equals unity. The overall projected area factors for diffuse radiation were obtained by integration of local quantities and are compared with the experimental results from various authors in Table 2.

Table 2 Comparison of predicted overall projected area factors for diffuse solar radiation with measured effective radiation area factors

Description	Effective radiation area factor			
	Standing posture		Sedentary posture	
	Nude	Clothed	Nude	Clothed
Present study	0.84		0.78	
Bedford[a]	0.82		0.72	
Guibert[b]	0.73		0.65	
Fanger[c]	0.73	0.87	0.7	0.77
Horikoshi[d]	0.8	0.91	0.74	0.8
Miyazaki[e]	0.83		0.78	
Tanabe[f]	0.74		0.69	

[a] Bedford (1935).
[b] Guiber and Taylor (1952).
[c] Fanger (1970).
[d] Horikoshi et al. (1990).
[e] Miyazaki et al. (1995).
[f] Tanabe et al. (2000).

The results of the present study agreed well (within 5% relative error) with data obtained by Bedford, Horikoshi and Miyazaki but they are greater (13% relative error) than those obtained, e.g. by Fanger and Tanabe. It is hypothesized that these discrepancies were due to differences in the body posture considered. In this study the geometry models for both the standing and sedentary posture represented relaxed, stress-free position. In contrast, other studies considered compact geometry models and subjects with extremities closely attached to each other or to the body.

While most investigations have dealt with the overall radiation characteristics of the human body, to date, also some information is available on measured local quantities. In Fig. 16, the predicted local projected area factors of individual body parts with respect to direct radiation are compared with the corresponding measured data obtain by Jones et al. (1998). To make a comparison pos-

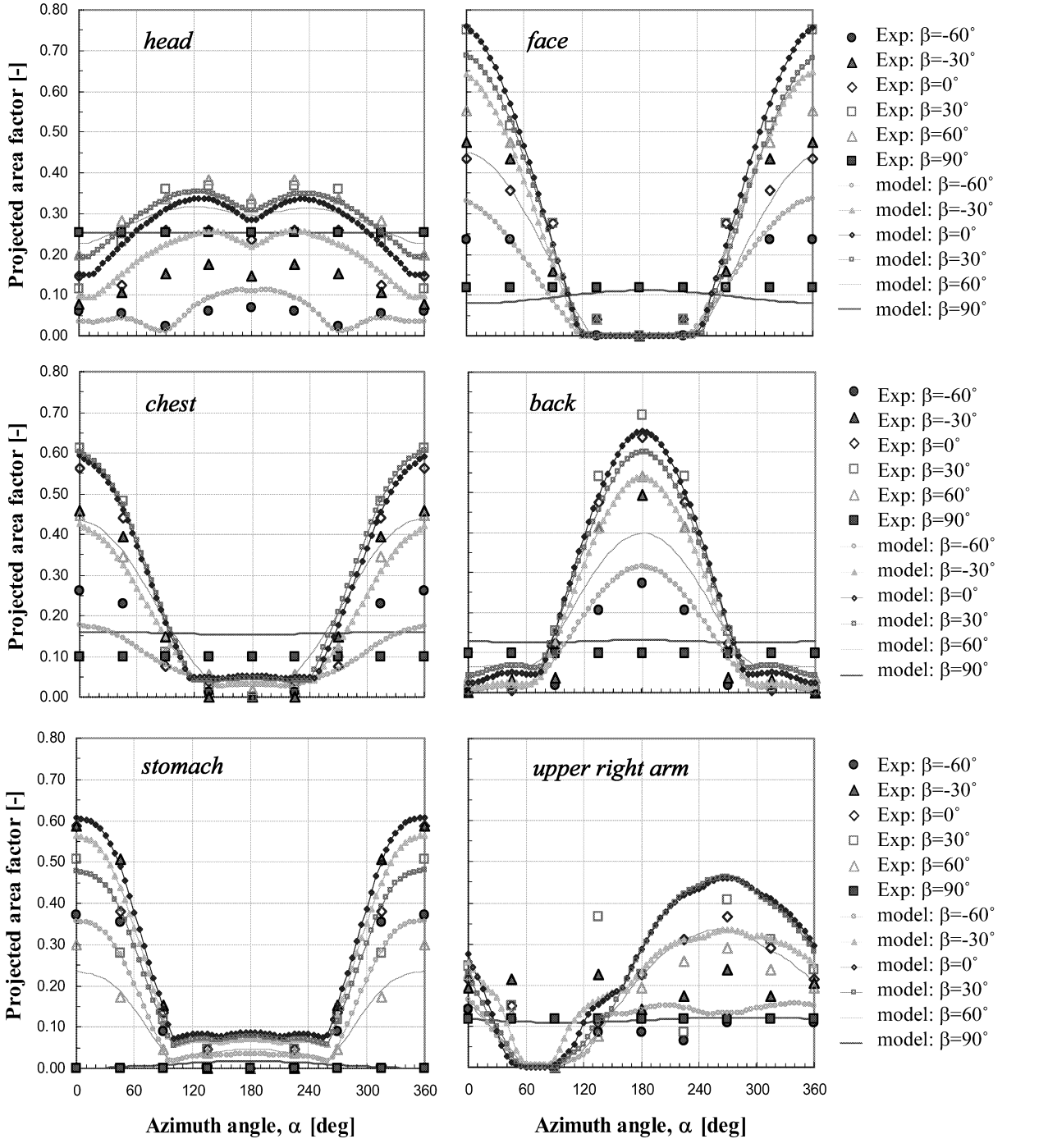

Fig. 16 Comparison of local projected area factors predicted for individual body parts with measured data using a standing manikin, Jones et al. (1998)

sible the predictions referring to individual spatial body sectors were integrated locally to obtain f_p-factors of the body parts according to the experimental set-up. Unfortunately, no experimental data were found with which to compare predicted local f_p-factors for diffuse radiation.

As in the case of overall factors, also the predicted local f_p-factors agreed generally well with the measurements reproducing both the trend and absolute values for most body sectors. The average deviation including all angles and body sectors was $\Delta f_p = \pm 0.03$. Partly large discrepancies however resulted for non-central body sectors such as feet. A thorough analysis of the results assumed that the discrepancies were most likely associated with the following differences between model and experiment.

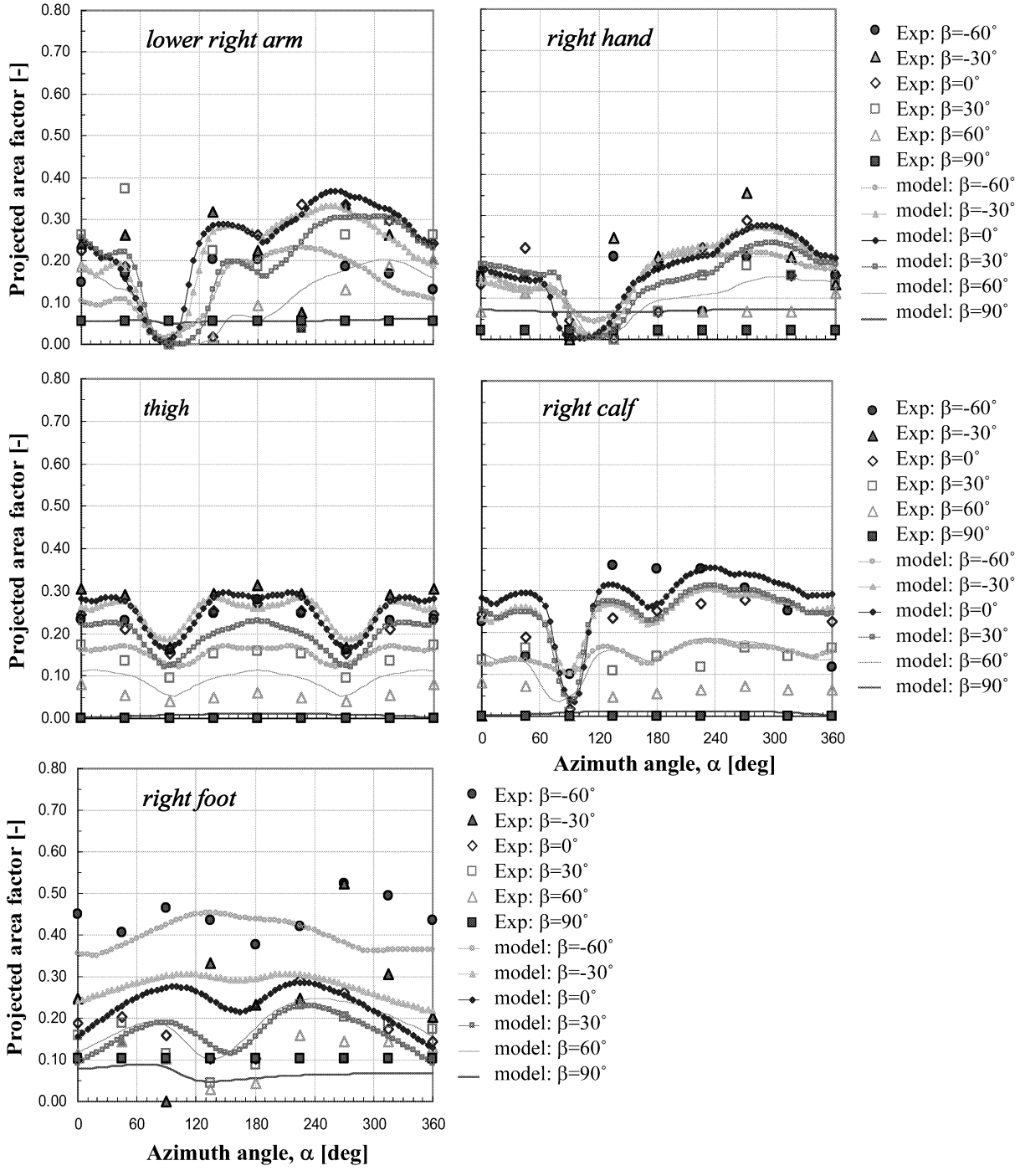

Fig. 16 (continued)

Besides differences in posture that were suggested to cause discrepancies between predicted and measured local f_p-values particularly in extremities, there were also some differences in the segmentation of the computer model and the manikin used in the trials.

However, the main point was probably that the simulations were performed for parallel rays with the high intensity source at an infinite distance from the human body but the experiments were conducted for finite distances between the body and the camera. In case of the Jones et al. experiment the distance was 4.3 m for positive altitude angles and 3.7 m for negative altitude angles, respectively. To this point the azimuth and the altitude angles of the camera were measured from the centre of the manikin. There was good agreement with the measured f_p-factors for body parts that were close to the body centre such as stomach and chest. For body parts such as head, face, upper arms and feet, however, a lower level

of agreement between prediction and experiment was achieved. This was because the position of the camera, i.e. the angles α and β, relative to the body centre, increasingly deviated from the position relative to the individual body parts, and thus from the direction of the parallel rays in the simulations.

Conclusion

In this study, regression equations for predicting local projected area factors of standing and sedentary persons were developed using detailed computer models of the human body geometry and numerical ray-tracing techniques. The new regression model was developed for both diffuse and direct solar radiation. Validation tests showed good general agreement with measured data for both overall and local quantities. Discrepancies between predicted and measured data appeared to be associated mainly with differences in posture and with the fact that the simulations were performed for parallel rays with the high intensity source being at an infinite distance from the body whereas the experiments were performed for finite distances.

The projected area factor equations developed in this study can be used to predict the irradiation and absorption of direct and diffuse solar radiation over the 3D surface of the human body. Bio-meteorologists and other scientists can use the equations to perform detailed analysis of the effect of solar radiation on human beings exposed to outdoor weather conditions. This information can serve, for example, to develop bio-climatic charts and rationally derived operative temperatures which characterise the outdoor climate conditions including the effect of solar radiation on humans.

The presented equations may prove useful especially when used in conjunction with detailed, multi-segmental models of the human thermoregulatory system and thermal comfort. With these models the thermal effect of direct and diffuse solar radiation on humans and the associated physiological and perceptual implications can be quantified. Another possible application of the equations, besides any thermal effects, is the prediction of the UV-dose and the assessment of the associated health risks and possible injuries to exposed body parts.

Appendix

Tables 3, 4, 5, 6, 7, 8, 9, 10

Table 3 Polynomial of the coefficient A of the basic cosine function f_p (Eq. 2), $A = \sum_{j=0}^{4} a_j \beta^j$ and the corresponding correlation coefficient, R

Body sectors	Standing posture						Sedentary posture					
	a_0	a_1	a_2	a_3	a_4	R	a_0	a_1	a_2	a_3	a_4	R
Head	0.1429	–0.0284	–0.0668	0.0169	0.0000	1.00	0.1486	–0.0300	–0.0682	0.0180	0.0000	1.00
Forehead	0.5055	0.0366	–0.2348	0.0000	0.0000	1.00	0.5144	0.0453	–0.2363	0.0000	0.0000	1.00
Face (anterior)	0.3178	–0.1671	0.0000	0.0891	–0.0695	0.97	0.3296	–0.1260	–0.0581	0.0720	–0.0455	0.99
Face (exterior)	0.8526	–0.0115	–0.4797	0.0294	0.0387	1.00	0.8551	–0.0012	–0.4913	0.0263	0.0440	1.00
Neck (anterior)	0.6988	–0.4388	–0.3071	0.1816	0.0000	0.99	0.7272	–0.4806	–0.4488	0.2446	0.0403	1.00
Neck (posterior)	0.5749	0.0429	–0.2468	0.0000	0.0000	0.98	0.6137	0.0391	–0.2692	0.0000	0.0000	0.99
Shoulder	0.1568	0.1954	–0.0481	–0.0925	0.0000	0.98	0.1591	0.1594	–0.0591	–0.0635	0.0000	0.98
Thorax (anterior)	0.5050	0.1582	–0.3273	–0.0674	0.0525	1.00	0.5334	0.2031	–0.3729	–0.0792	0.0667	1.00
Thorax (posterior)	0.5196	0.0257	–0.3047	–0.0157	0.0423	1.00	0.5371	0.0117	–0.3084	–0.0064	0.0414	1.00
Abdomen (anterior)	0.7090	–0.1368	–0.3400	0.0436	0.0268	1.00	0.4966	0.2208	–0.4061	–0.0978	0.0915	0.99
Abdomen (posterior)	0.4876	0.0406	–0.2671	–0.0241	0.0349	1.00	0.4521	–0.0384	–0.1954	0.0203	0.0000	1.00
Upper arm (anterior)	0.5678	–0.0414	–0.3145	0.0000	0.0445	1.00	0.6135	–0.0953	–0.2806	0.0528	0.0000	0.99
Upper arm (posterior)	0.5043	0.0159	–0.2148	0.0000	0.0000	1.00	0.4584	–0.2358	–0.2009	0.1005	0.0000	0.99
Lower arm (anterior)	0.7318	0.0920	–0.3252	–0.0212	0.0000	1.00	0.5710	0.0575	–0.2563	0.0000	0.0000	0.99
Lower arm (posterior)	0.6152	–0.1644	–0.3402	0.0655	0.0350	1.00	0.3652	–0.2153	–0.2808	0.0915	0.0553	0.99
Hand (handback)	0.3494	–0.0305	–0.1566	0.0215	0.0000	0.99	0.7875	–0.1788	–0.5674	0.0709	0.1011	1.00
Hand (palm)	0.2782	0.0000	–0.1165	0.0000	0.0000	0.98	0.1195	0.0135	–0.0542	0.0000	0.0000	0.97
Upper leg (anterior)	0.7597	0.0251	–0.4238	0.0000	0.0378	1.00	0.1071	–0.0388	–0.0725	0.0108	0.0161	0.81
Upper leg (posterior)	0.5509	–0.0317	–0.2739	0.0124	0.0200	1.00	0.6481	0.0402	–0.2499	–0.0124	–0.0050	0.95
Lower leg (anterior)	0.6848	0.0000	–0.3028	0.0000	0.0000	0.96	0.1749	–0.2020	–0.0804	0.0917	0.0000	0.98
Lower leg (posterior)	0.4285	0.0258	–0.2241	–0.0132	0.0238	1.00	0.5785	0.0000	–0.3114	0.0000	0.0348	0.99
Foot (instep)	0.1720	0.1009	0.1104	–0.0441	–0.0715	0.88	0.3552	–0.0665	–0.2435	0.0208	0.0449	1.00

Table 4 Polynomial of the coefficient B of the basic cosine function f_p (Eq. 2), $B = \sum_{j=0}^{4} b_j \beta^j$ and the corresponding correlation coefficient, R

Body sectors	Standing posture						Sedentary posture					
	b_0	b_1	b_2	b_3	b_4	R	b_0	b_1	b_2	b_3	b_4	R
Head	0.2575	0.1362	−0.0322	0.0000	0.0000	1.00	0.2573	0.1335	−0.0319	0.0000	0.0000	1.00
Forehead	0.2667	0.0005	−0.1139	0.0196	0.0059	1.00	0.2728	0.0000	−0.1037	0.0248	0.0000	1.00
Face (anterior)	0.2852	0.0000	−0.2266	0.0000	0.0474	0.98	0.2782	−0.0430	−0.1675	0.0386	0.0123	1.00
Face (exterior)	0.0689	−0.0528	−0.0336	0.0285	0.0000	0.92	0.0692	−0.0416	−0.0350	0.0245	0.0000	0.92
Neck (anterior)	0.1264	0.0394	−0.2067	0.0780	0.0000	0.98	0.1203	0.1017	−0.1350	0.0000	0.0000	0.96
Neck (posterior)	0.3219	0.2376	−0.1510	−0.0897	0.0000	0.95	0.2891	0.2264	−0.1319	−0.0879	0.0000	0.96
Shoulder	0.1891	0.4127	0.0883	−0.0722	0.0000	0.99	0.1839	0.4316	0.0890	−0.0796	0.0000	0.99
Thorax (anterior)	0.2421	0.0703	−0.0625	0.0000	0.0000	0.97	0.2586	0.0996	−0.0914	0.0000	0.0000	0.92
Thorax (posterior)	0.3539	0.0000	−0.1895	0.0000	0.0390	0.98	0.3694	0.0000	−0.1842	0.0000	0.0342	1.00
Abdomen (anterior)	0.1325	0.0000	−0.1112	0.0000	0.0251	0.95	0.0889	0.0000	−0.0635	0.0000	0.0144	0.96
Abdomen (posterior)	0.2934	0.0000	−0.1057	−0.0088	0.0000	0.99	0.3658	−0.1778	−0.0899	0.0312	0.0000	1.00
Upper arm (anterior)	0.2420	−0.0387	−0.1203	0.0321	0.0000	1.00	0.1862	−0.0851	−0.0806	0.0373	0.0000	0.97
Upper arm (posterior)	0.3284	0.0180	−0.2176	0.0000	0.0445	0.99	0.2732	0.0531	−0.0837	0.0000	0.0000	0.98
Lower arm (anterior)	0.1510	0.1367	−0.0819	0.0000	0.0000	0.99	0.2673	0.2509	−0.1383	0.0000	0.0000	0.97
Lower arm (posterior)	0.3051	−0.1363	−0.1757	0.0164	0.0479	1.00	0.1338	−0.2768	0.0505	0.0538	0.0000	0.99
Hand (handback)	0.1967	−0.0477	−0.0151	0.0000	0.0000	0.98	0.2414	0.2629	0.0265	−0.0413	0.0000	0.99
Hand (palm)	0.1613	0.0000	−0.0431	0.0000	0.0000	0.97	0.0880	−0.0659	−0.0055	0.0143	0.0000	0.97
Upper leg (anterior)	0.1033	−0.0419	−0.0271	0.0139	0.0000	0.95	0.0801	0.2316	0.1675	−0.0261	−0.0406	1.00
Upper leg (posterior)	0.3457	−0.0614	−0.1973	0.0133	0.0210	1.00	0.1455	−0.4860	0.1043	0.0533	0.0000	0.97
Lower leg (anterior)	0.1902	0.0000	−0.0991	0.0000	0.0000	0.78	0.2683	0.1251	−0.0696	−0.0290	−0.0052	0.98
Lower leg (posterior)	0.3663	0.0173	−0.1646	−0.0094	0.0097	1.00	0.3262	−0.0605	−0.2212	0.0117	0.0451	1.00
Foot (instep)	0.2021	0.1090	−0.0354	−0.0407	0.0000	0.91	0.3302	0.2096	−0.0540	−0.0506	0.0000	1.00

Table 5 Polynomial of the coefficients C_0, C_1 (order 1) of the basic cosine function f_p (Eq. 2) and the corresponding correlation coefficient, R

Body sectors	Standing posture						Sedentary posture					
	c_{00}	c_{01}	R	c_{10}	c_{11}	R	c_{00}	c_{01}	R	c_{10}	c_{11}	R
Head	3.2183	−0.0758	0.35	−1.0279	0.0107	0.19	3.2715	−0.1356	0.53	−1.0446	0.0386	0.57
Forehead	0.1762	−0.1081	0.75	0.9432	0.0086	0.79	0.1730	−0.1101	0.74	0.9583	0.0119	0.89
Face (anterior)	0.1034	0.0510	0.82	0.9705	−0.0137	0.66	0.0946	0.0424	0.67	0.9811	0.0101	0.33
Face (exterior)	1.4099	−0.0276	0.73	−0.9990	0.0053	0.42	1.4096	−0.0142	0.40	−1.0014	−0.0033	0.66
Neck (anterior)	0.1090	−0.3044	0.89	0.9757	0.0795	0.81	0.0866	−0.2052	0.65	0.9928	0.0828	0.74
Neck (posterior)	3.9317	−0.1531	0.85	−1.2544	0.0485	0.82	3.9576	−0.2507	0.92	−1.2604	0.0763	0.93
Shoulder	2.5542	−0.7017	0.87	−1.0917	0.1903	0.92	2.6405	−0.4897	0.89	−1.1059	0.1347	0.91
Thorax (anterior)	0.2254	−0.0646	0.36	0.9257	0.0371	0.41	0.1823	−0.0260	0.19	0.9414	0.0525	0.77
Thorax (posterior)	3.9443	−0.1067	0.72	−1.2474	0.0362	0.73	3.9725	−0.0702	0.55	−1.2560	0.0241	0.57
Abdomen (anterior)	0.0311	0.0496	0.99	0.9939	−0.0167	0.98	0.3130	−0.3398	0.93	0.9141	0.0886	0.96
Abdomen (posterior)	3.7547	0.1105	0.75	−1.1960	−0.0328	0.74	3.8124	0.2800	0.99	−1.2112	−0.0954	0.98
Upper arm (anterior)	0.0441	−0.0360	0.88	0.9534	−0.0223	0.65	0.1824	−0.0975	0.96	0.9441	−0.0530	0.75
Upper arm (posterior)	3.4855	−0.2381	0.91	−1.2105	0.0413	0.87	2.8236	−0.1378	0.97	−1.1151	0.0588	0.80
Lower arm (anterior)	0.3282	0.0110	0.34	0.9847	−0.0029	0.42	1.4804	−0.0573	0.27	1.0000	0.0000	1.00
Lower arm (posterior)	3.2771	0.2552	0.91	−1.1789	−0.0927	0.92	1.8367	0.0566	0.71	−1.0269	−0.0412	0.86
Hand (handback)	1.2449	−0.1577	0.98	−1.0007	−0.0336	0.86	1.9315	−0.8627	0.95	−1.0090	0.0238	0.62
Hand (palm)	−4.4198	0.0184	0.26	1.0311	−0.0200	0.58	2.5396	0.7663	0.73	−1.0254	−0.1099	0.86
Upper leg (anterior)	0.2113	0.0786	0.93	0.9631	−0.0282	0.80	1.4677	−0.3523	0.88	0.8350	0.1600	0.92
Upper leg (posterior)	3.9764	0.1252	0.93	−1.2570	−0.0607	0.98	1.9333	0.2783	0.87	−0.9937	−0.2803	0.95
Lower leg (anterior)	0.1308	−0.0273	0.40	0.9623	−0.0080	0.55	0.2054	0.0719	0.73	0.9737	−0.0359	0.90
Lower leg (posterior)	3.7871	−0.0460	0.56	−1.1793	0.0035	0.14	3.6365	0.3189	0.88	−1.1438	−0.1025	0.86
Foot (instep)	2.3696	−0.9467	0.97	−0.7118	0.2209	0.98	2.5856	−0.0340	0.22	−0.8540	−0.0271	0.28

Table 6 Polynomial of the coefficient D_1 of the shading function S (Eq. 7), $D_1 = \sum_{j=0}^{4} d_{1j}\beta^j$ and the corresponding correlation coefficient, R

Body sectors	Standing posture						Sedentary posture					
	d_{10}	d_{11}	d_{12}	d_{13}	d_{14}	R	d_{10}	d_{11}	d_{12}	d_{13}	d_{14}	R
Head	0.0000	0.0000	2.1243	−1.4816	0.0000	0.98	0.0000	0.0000	2.2067	−1.5336	0.0000	0.99
Forehead	0.0000	0.0000	0.0000	0.0000	0.0000	1.00	0.6670	0.0000	−3.7470	3.2480	−0.6164	0.98
Face (anterior)	0.0000	0.0000	0.0000	0.0000	0.0000	1.00	4.6866	0.0000	−2.7218	5.3366	−2.5000	0.99
Face (exterior)	0.1494	0.0000	−0.3568	1.5754	−0.9315	0.99	0.2106	0.0000	−0.8538	1.6030	−0.7353	0.99
Neck (anterior)	0.0000	0.0000	0.0000	0.0000	0.0000	1.00	2.6061	0.0000	−2.5611	4.4336	−1.9472	0.99
Neck (posterior)	0.0000	0.0000	0.0000	0.0000	0.0000	1.00	0.0000	0.0000	0.0000	0.0000	0.0000	1.00
Shoulder	−1.0723	−1.9802	3.7159	−4.7018	2.1357	0.68	−1.0341	−3.3306	6.8021	−7.1132	2.7330	0.89
Thorax (anterior)	0.0000	0.0000	0.0000	0.0000	0.0000	1.00	0.4153	−0.2248	−1.5944	1.0646	0.0000	0.98
Thorax (posterior)	0.0000	0.0000	0.0000	0.0000	0.0000	1.00	0.0000	0.0000	0.0000	0.0000	0.0000	1.00
Abdomen (anterior)	0.0000	0.0000	0.0000	0.0000	0.0000	1.00	1.3969	2.0986	−9.7482	5.2014	0.0000	0.99
Abdomen (posterior)	0.0000	0.0000	0.0000	0.0000	0.0000	1.00	0.0000	0.0000	0.0000	0.0000	0.0000	1.00
Upper arm (anterior)	−1.8501	2.7489	−4.4776	−3.1264	3.4099	0.86	−0.9564	1.1929	−1.6068	0.0000	0.0000	0.97
Upper arm (posterior)	0.0000	0.0000	0.0000	0.0000	0.0000	1.00	0.0000	0.0000	0.0000	0.0000	0.0000	1.00
Lower arm (anterior)	−3.1354	−1.7318	1.1750	0.4795	0.0000	0.97	−0.5390	−0.5152	−0.5088	0.0000	0.0000	0.74
Lower arm (posterior)	0.1584	1.0956	−2.0176	0.0000	0.0000	0.83	0.0000	0.0000	0.0000	0.0000	0.0000	1.00
Hand (handback)	0.0502	−0.1554	−0.2115	0.5317	−0.2105	0.99	−1.0267	−0.3723	−1.5312	0.0000	0.9131	0.93
Hand (palm)	−2.9380	−0.9203	−0.7716	0.5989	0.7053	0.90	0.0000	0.0000	0.0000	0.0000	0.0000	1.00
Upper leg (anterior)	0.0000	0.0000	0.0000	0.0000	0.0000	1.00	−2.1922	−2.8941	2.5620	0.0000	0.0000	0.75
Upper leg (posterior)	0.0000	0.0000	0.0000	0.0000	0.0000	1.00	−0.1230	−2.9899	3.0351	1.9843	−1.2342	0.91
Lower leg (anterior)	4.5282	18.1753	15.9558	0.0000	0.0000	1.00	0.0000	0.0000	0.0000	0.0000	0.0000	1.00
Lower leg (posterior)	−8.4381	−1.4005	3.5985	0.0000	0.0000	0.85	−1.7804	−6.3434	−3.5564	0.0000	0.0000	0.99
Foot (instep)	−1.6535	−0.0277	0.4633	0.0000	0.0000	0.82	−0.8878	−0.5349	0.1774	0.0000	0.0000	0.99

Table 7 Polynomial of the coefficient D_0 of the shading function S (Eq. 7), $D_0 = \sum_{j=0}^{4} d_{0j}\beta^j$ and the corresponding correlation coefficient, R

Body sectors	Standing posture						Sedentary posture					
	d_{00}	d_{01}	d_{02}	d_{03}	d_{04}	R	d_{00}	d_{01}	d_{02}	d_{03}	d_{04}	R
Head	10.3361	0.0000	−3.5647	7.9337	−3.7827	1.00	10.4314	0.0000	−4.3398	7.9768	−3.4768	1.00
Forehead	10.0000	0.0000	0.0000	0.0000	0.0000	1.00	10.4341	0.0000	−1.3449	4.0352	−2.1992	0.99
Face (anterior)	9.4813	0.0000	0.0000	1.9329	−1.1810	0.99	10.5145	0.0000	−2.1120	3.8723	−1.7547	0.99
Face (exterior)	9.8010	0.0000	−2.1483	2.5356	−0.6751	0.99	9.7467	0.0000	−1.7072	2.5111	−0.8491	1.00
Neck (anterior)	10.0000	0.0000	0.0000	0.0000	0.0000	1.00	10.5755	0.0000	−2.5097	4.0732	−1.7210	0.99
Neck (posterior)	10.0000	0.0000	0.0000	0.0000	0.0000	1.00	10.0000	0.0000	0.0000	0.0000	0.0000	1.00
Shoulder	10.3034	−26.4505	56.1918	−38.1416	6.9506	0.74	4.1224	6.3639	−6.0508	9.1870	−5.2962	0.89
Thorax (anterior)	10.0000	0.0000	0.0000	0.0000	0.0000	1.00	11.6820	−0.7202	−6.6952	4.3811	0.0000	0.99
Thorax (posterior)	10.0000	0.0000	0.0000	0.0000	0.0000	1.00	10.0000	0.0000	0.0000	0.0000	0.0000	1.00
Abdomen (anterior)	10.0000	0.0000	0.0000	0.0000	0.0000	1.00	10.8156	3.0347	−9.1398	4.5321	0.0000	0.99
Abdomen (posterior)	10.0000	0.0000	0.0000	0.0000	0.0000	1.00	10.0000	0.0000	0.0000	0.0000	0.0000	1.00
Upper arm (anterior)	6.0537	−10.8155	13.1404	9.7346	−9.8565	0.87	2.4926	−3.2681	3.9089	0.0000	0.0000	0.98
Upper arm (posterior)	10.0000	0.0000	0.0000	0.0000	0.0000	1.00	10.0000	0.0000	0.0000	0.0000	0.0000	1.00
Lower arm (anterior)	5.2125	2.4462	−1.4207	0.0000	0.0000	0.90	0.3278	0.8296	3.0252	0.0000	0.0000	0.90
Lower arm (posterior)	10.0379	−3.1011	3.8970	0.0000	0.0000	0.73	10.0000	0.0000	0.0000	0.0000	0.0000	1.00
Hand (handback)	11.0207	0.0960	−7.5119	1.7539	4.5080	0.79	2.2893	1.6263	2.0569	0.0000	0.0000	1.00
Hand (palm)	11.0700	3.0451	1.0763	−1.8525	−1.4769	0.73	10.0000	0.0000	0.0000	0.0000	0.0000	1.00
Upper leg (anterior)	10.0000	0.0000	0.0000	0.0000	0.0000	1.00	7.8801	−9.0053	6.7207	0.0000	0.0000	0.91
Upper leg (posterior)	10.0000	0.0000	0.0000	0.0000	0.0000	1.00	1.2488	5.7338	2.7077	−1.6714	0.0000	0.98
Lower leg (anterior)	24.2222	21.2884	0.0000	0.0000	0.0000	0.99	10.0000	0.0000	0.0000	0.0000	0.0000	1.00
Lower leg (posterior)	37.8126	5.1634	−12.9276	0.0000	0.0000	0.80	9.8134	5.4458	17.6432	0.0000	0.0000	1.00
Foot (instep)	5.1013	0.1025	−1.0893	0.0000	0.0000	0.79	2.0440	1.5734	−0.3840	0.0000	0.0000	0.99

Table 8 Polynomial of the coefficient E_1 of the shading function S (Eq. 7), $E_1 = \sum_{j=0}^{4} e_{1j}\beta^j$ and the corresponding correlation coefficient, R

Body sectors	Standing posture						Sedentary posture					
	e_{10}	e_{11}	e_{12}	e_{13}	e_{14}	R	e_{10}	e_{11}	e_{12}	e_{13}	e_{14}	R
Head	0.0000	0.0000	0.0000	0.0000	0.0000	1.00	0.0000	0.0000	0.0000	0.0000	0.0000	1.00
Forehead	0.0000	0.0000	0.0000	0.0000	0.0000	1.00	−0.4162	0.0000	1.5095	−3.4811	1.7460	0.99
Face (anterior)	0.0000	0.0000	0.0000	0.0000	0.0000	1.00	−2.3848	0.0000	1.5508	−2.9470	1.3599	0.99
Face (exterior)	−0.1427	0.0000	0.7756	−0.7405	0.1746	0.98	−0.1022	0.0000	0.4464	−0.7221	0.3045	0.99
Neck (anterior)	0.0000	0.0000	0.0000	0.0000	0.0000	1.00	−0.3483	0.0000	1.3525	−2.7572	1.3150	0.99
Neck (posterior)	0.0000	0.0000	0.0000	0.0000	0.0000	1.00	0.0000	0.0000	0.0000	0.0000	0.0000	1.00
Shoulder	0.0210	6.8935	−7.1246	2.2240	−0.2474	0.98	1.9987	−5.1473	26.6276	−28.0890	8.1664	1.00
Thorax (anterior)	0.0000	0.0000	0.0000	0.0000	0.0000	1.00	−0.3641	0.1502	1.4563	−0.9504	0.0000	0.99
Thorax (posterior)	0.0000	0.0000	0.0000	0.0000	0.0000	1.00	0.0000	0.0000	0.0000	0.0000	0.0000	1.00
Abdomen (anterior)	0.0000	0.0000	0.0000	0.0000	0.0000	1.00	−0.3302	−0.9457	3.1923	−1.6228	0.0000	0.99
Abdomen (posterior)	0.0000	0.0000	0.0000	0.0000	0.0000	1.00	0.0000	0.0000	0.0000	0.0000	0.0000	1.00
Upper arm (anterior)	5.5679	1.9454	−1.2164	−1.8151	0.2334	1.00	6.0685	3.0772	−2.6042	0.0000	0.0000	0.72
Upper arm (posterior)	0.0000	0.0000	0.0000	0.0000	0.0000	1.00	0.0000	0.0000	0.0000	0.0000	0.0000	1.00
Lower arm (anterior)	5.9843	1.6183	−1.9134	0.0000	0.0000	0.97	4.1228	−4.0001	2.0945	0.0000	0.0000	1.00
Lower arm (posterior)	−0.2635	0.0000	0.0000	−1.2257	0.8901	0.93	0.0000	0.0000	0.0000	0.0000	0.0000	1.00
Hand (handback)	−0.2466	0.1938	1.6008	−1.0277	−0.5032	0.97	4.4608	1.8997	1.3831	0.0000	−1.7785	0.99
Hand (palm)	6.2294	4.2117	−3.6825	−3.0284	1.2923	0.94	0.0000	0.0000	0.0000	0.0000	0.0000	1.00
Upper leg (anterior)	0.0000	0.0000	0.0000	0.0000	0.0000	1.00	1.7368	4.8871	−3.8096	0.0000	0.0000	0.99
Upper leg (posterior)	0.0000	0.0000	0.0000	0.0000	0.0000	1.00	4.4658	0.0000	−4.1471	0.0000	0.0000	0.99
Lower leg (anterior)	0.0000	0.0000	0.0000	0.0000	0.0000	1.00	0.0000	0.0000	0.0000	0.0000	0.0000	1.00
Lower leg (posterior)	6.6866	0.7040	−2.8396	0.0000	0.0000	0.91	0.3438	1.6788	0.8795	0.0000	0.0000	0.98
Foot (instep)	1.2117	0.1377	0.4531	0.0000	0.0000	0.53	0.7784	−0.2893	0.3042	0.0000	0.0000	0.92

Table 9 Polynomial of the coefficient E_0 of the shading function S (Eq. 7), $E_0 = \sum_{j=0}^{4} e_{0j}\beta^j$ and the corresponding correlation coefficient, R

Body sectors	Standing posture						Sedentary posture					
	e_{00}	e_{01}	e_{02}	e_{03}	e_{04}	R	e_{00}	e_{01}	e_{02}	e_{03}	e_{04}	R
Head	−10.0000	0.0000	0.0000	0.0000	0.0000	1.00	−10.0000	0.0000	0.0000	0.0000	0.0000	1.00
Forehead	−10.0000	0.0000	0.0000	0.0000	0.0000	1.00	−10.3862	0.0000	1.5419	−2.9823	1.3881	0.99
Face (anterior)	−10.0000	0.0000	0.0000	0.0000	0.0000	1.00	−10.4127	0.0000	1.6100	−3.2543	1.5461	0.99
Face (exterior)	−10.2218	0.0000	0.4719	−2.4400	1.4776	0.99	−10.3251	0.0000	1.3117	−2.4867	1.1462	0.99
Neck (anterior)	−10.0000	0.0000	0.0000	0.0000	0.0000	1.00	−8.4190	0.0000	−6.4429	11.9803	−5.4684	0.99
Neck (posterior)	−10.0000	0.0000	0.0000	0.0000	0.0000	1.00	−10.0000	0.0000	0.0000	0.0000	0.0000	1.00
Shoulder	−10.1151	25.8754	−90.9687	92.9137	−27.7784	0.96	−10.0158	32.1237	−166.178	178.165	−53.2005	1.00
Thorax (anterior)	−10.0000	0.0000	0.0000	0.0000	0.0000	1.00	−11.4243	0.0000	5.7636	−3.4827	0.0000	0.98
Thorax (posterior)	−10.0000	0.0000	0.0000	0.0000	0.0000	1.00	−10.0000	0.0000	0.0000	0.0000	0.0000	1.00
Abdomen (anterior)	−10.0000	0.0000	0.0000	0.0000	0.0000	1.00	−10.9460	−3.2629	10.1397	−5.0642	0.0000	0.99
Abdomen (posterior)	−10.0000	0.0000	0.0000	0.0000	0.0000	1.00	−10.0000	0.0000	0.0000	0.0000	0.0000	1.00
Upper arm (anterior)	−32.1692	−11.3790	12.9772	11.0889	−5.5058	0.99	−33.3682	−20.3675	10.4118	8.6932	0.0000	0.84
Upper arm (posterior)	−10.0000	0.0000	0.0000	0.0000	0.0000	1.00	−10.0000	0.0000	0.0000	0.0000	0.0000	1.00
Lower arm (anterior)	−30.6274	−8.9154	10.2034	0.0000	0.0000	0.99	−19.5739	14.3501	−5.7091	0.0000	0.0000	1.00
Lower arm (posterior)	−8.8667	0.0000	0.0000	5.2726	−3.8289	0.93	−10.0000	0.0000	0.0000	0.0000	0.0000	1.00
Hand (handback)	−10.3122	−0.5993	2.8599	1.0495	−2.9175	0.99	−22.6841	−2.2215	−6.8150	6.3853	0.0000	0.98
Hand (palm)	−31.3503	−19.9270	24.5164	14.5318	−10.8305	0.94	−10.0000	0.0000	0.0000	0.0000	0.0000	1.00
Upper leg (anterior)	−10.0000	0.0000	0.0000	0.0000	0.0000	1.00	−8.1428	−12.4157	8.9144	0.0000	0.0000	0.86
Upper leg (posterior)	−10.0000	0.0000	0.0000	0.0000	0.0000	1.00	−17.6655	1.0177	2.0342	0.0000	0.0000	0.90
Lower leg (anterior)	−10.0000	0.0000	0.0000	0.0000	0.0000	1.00	−10.0000	0.0000	0.0000	0.0000	0.0000	1.00
Lower leg (posterior)	−38.5826	−2.3193	13.7304	0.0000	0.0000	0.81	−2.7314	0.0000	−7.6802	−3.5505	0.0000	0.97
Foot (instep)	−4.3581	−1.1838	−2.3067	0.0000	0.0000	0.72	−3.0855	1.3211	−0.9556	0.0000	0.0000	0.88

Table 10 Polynomial of the coefficients g_0, g_1 of the $f_{p,dif}$ function for the diffuse shortwave radiation (Eq. 8) and the corresponding correlation coefficient, R

Body sectors	Standing posture			Sedentary posture		
	g_0	g_1	R	g_0	g_1	R
Head	0.6460	0.3183	1.00	0.6423	0.3211	1.00
Forehead	0.5194	0.4675	1.00	0.5295	0.4495	1.00
Face (anterior)	0.3701	0.4716	1.00	0.3777	0.4465	1.00
Face (exterior)	0.4318	0.4588	1.00	0.4354	0.4488	1.00
Neck (anterior)	0.3425	0.4367	1.00	0.3532	0.4137	1.00
Neck (posterior)	0.5783	0.3650	1.00	0.5671	0.3757	1.00
Shoulder	0.8119	0.0927	1.00	0.7982	0.0866	1.00
Thorax (anterior)	0.5603	0.3711	1.00	0.5723	0.3399	1.00
Thorax (posterior)	0.4850	0.4739	1.00	0.4892	0.4995	1.00
Abdomen (anterior)	0.3970	0.4954	1.00	0.3101	0.1801	1.00
Abdomen (posterior)	0.4328	0.4558	1.00	0.4025	0.7381	1.00
Upper arm (anterior)	0.3505	0.4036	1.00	0.2165	0.2585	1.00
Upper arm (posterior)	0.4745	0.4576	1.00	0.5701	0.4464	1.00
Lower arm (anterior)	0.5132	0.3639	1.00	0.3529	0.0726	1.00
Lower arm (posterior)	0.3473	0.6165	1.00	0.3101	0.7620	1.00
Hand (handback)	0.3966	0.4861	1.00	0.6053	0.1090	1.00
Hand (palm)	0.1879	0.1894	1.00	0.0757	0.1787	1.00
Upper leg (anterior)	0.4106	0.4619	1.00	0.6037	0.1081	1.00
Upper leg (posterior)	0.4181	0.5203	1.00	0.3131	0.4627	1.00
Lower leg (anterior)	0.4374	0.4898	1.00	0.2558	0.3077	1.00
Lower leg (posterior)	0.4673	0.4728	1.00	0.4269	0.4972	1.00
Foot (instep)	0.5608	0.3005	1.00	0.3663	0.3743	1.00

References

Bedford T (1935) The effective radiating surface of the human body. J Hyg Camb 35:303–306

Blazejczyk K (1996) Assessment of solar radiation absorbed by man based on simple meteorological parameters, 7th International Conference on Environmental Ergonomics, Israel, Conference proceedings

Blazejczyk K, Nilsson H, Holmer I (1992) A modified equation for the calculation of solar heat load in man, 5th International Conference on Environmental Ergonomics, Maastricht, Conference proceedings

Breckenridge JR, Goldman RF (1972) Human solar heat load. ASHRAE, Trans 78(1):110–119

Curious Labs (2000) POSER4: the premier 3D character animation and figure design tool. Curious Labs, Santa Cruz

DuBois D, DuBois EF (1916) A formula to estimate approximate surface area, if height and weight are known. Arch Intern Med 17:863–871

Fanger PO (1970) Thermal comfort. McGraw-Hill, New York

Fiala D, Lomas KJ, Stohrer M (1999) A computer model of human thermoregulation for a wide range of environmental conditions: the passive system. J Appl Physiol 87:1957–1972

Fiala D, Lomas KJ, Stohrer M (2001) Computer prediction of human thermoregulatory and temperature responses to a wide range of environmental conditions. Int J Biometeorol 45:143–159

Fiala D, Lomas KJ, Stohrer M (2003) First principles modelling of thermal sensation responses in steady state and transient conditions. ASHRAE Trans 109:179–186

Guibert A, Taylor CL (1952) Radiation area of the human body. J Appl Physiol 5:24–37

Horikoshi T, Tsuchikawa T, Kobayashi Y, Miwa E, Kurazumi Y, Hirayama K (1990) The effective radiation area and angle factor between man and a rectangular plane near him. ASHRAE Trans 96(1):60–66

Huizenga C, Hui Z, Arens E (2001) A model of human physiology and comfort for assessing complex thermal environments. Building Environ 36:691–699

Jones BW, Hong S, McCullough EA (1998) Detailed projected area data for the human body. ASHRAE Trans 104(2):1327–1339

Kimlin M, Prisi A, Carter B, Turnbull D (2002) Comparison of the solar spectral ultraviolet irradiance in motor vehicles with windows in an open and closed position. Int J Biometeorol 46(3):150–156

Miyazaki Y, Saito M, Seshimo Y (1995) A study of evaluation non-uniform environments by human body model. J Hum Living Environ 2(1):92–100

Rizzo G, Franzitta G, Cannistraro G (1991) Algorithms for the calculation of the mean projected area of seated and standing persons. Energy and Buildings 17:221–230

Steinman M, Kalisperis LN, Summers LH (1988) Angle factor determination from a person to inclined surfaces. ASHRAE Trans 94(1):1809–1823

Stolwijk JAJ (1971) A mathematical model of physiological and behavioural temperature regulation in man. NASA contractor report CR-1855. NASA, Washington

Tanabe S, Narita C, Ozeki Y, Konishi M (2000) Effective radiation area of human body calculated by a numerical simulation. Energy and Buildings 32:205–215

ThermoAnalytics (2001) RadTherm Technical Documentation. Thermo Analytics, Calumet

Underwood CR, Ward EJ (1966) The solar radiation area of man. Ergonomics 9:155–168